

1     **Interhemispheric Influence of the Northern Summer Monsoons on the**  
2                     **Southern Subtropical Anticyclones**

3  
4  
5  
6  
7             Sang-Ki Lee<sup>1,2</sup>, Carlos R. Mechoso<sup>3</sup>, Chunzai Wang<sup>2</sup>, and J. David Neelin<sup>3</sup>

8             <sup>1</sup>Cooperative Institute for Marine and Atmospheric Studies, University of Miami, Miami FL

9             <sup>2</sup>Atlantic Oceanographic and Meteorological Laboratory, NOAA, Miami FL

10            <sup>3</sup>Department of Atmospheric and Oceanic Sciences, University of California, Los Angeles, Los  
11                                     Angeles, CA

12  
13  
14  
15  
16  
17  
18             Revised and resubmitted to Journal of Climate (2nd revision)

19                                     August 2013

20  
21  
22     Corresponding author address: Dr. Sang-Ki Lee, NOAA/AOML, 4301 Rickenbacker Causeway,

23     Miami, FL 33149, USA. E-mail: [Sang-Ki.Lee@noaa.gov](mailto:Sang-Ki.Lee@noaa.gov).

1 **Abstract**

2 The southern subtropical anticyclones are notably stronger in the austral winter than in  
3 summer, particularly over the Atlantic and Indian Ocean basins. This is in contrast with the  
4 Northern Hemisphere (NH), in which subtropical anticyclones are more intense in summer  
5 according to the “monsoon heating” paradigm. To better understand the winter intensification of  
6 southern subtropical anticyclones, the present study explores the interhemispheric response to  
7 monsoon heating in the NH during the austral winter. A specially designed suite of numerical  
8 model experiments is performed in which summer monsoons in the NH are artificially  
9 weakened. These experiments are performed with both an atmospheric general circulation model  
10 and a simple two-layer model. The highlight of our findings is that during the boreal summer  
11 enhanced tropical convection activity in the NH plays important roles in either maintaining or  
12 strengthening the southern subtropical anticyclones. Enhanced NH convection largely associated  
13 with the major summer monsoons produces subsidence over the equatorial oceans and the  
14 tropical Southern Hemisphere via interhemispheric meridional overturning circulations and  
15 increases the sea level pressure locally. In addition, suppressed convection over some regions of  
16 climatological subsidence produces stationary barotropic Rossby waves that propagate far  
17 beyond the tropics. These stationary barotropic Rossby waves and those forced directly by the  
18 summer heating in the NH are spatially phased to strengthen the southern subtropical  
19 anticyclones over all three oceans. The interhemispheric response to the NH summer monsoons  
20 is most dramatic in the South Pacific, where the subtropical anticyclone nearly disappears in the  
21 austral winter without the influence from the NH.

1 **1. Introduction**

2 In our current understanding, the principal driver of the subtropical anticyclones (also known  
3 as the subtropical highs) varies with season. This principal driver is heating associated with the  
4 monsoons over the adjacent continents during the summer season, and orographic effects on the  
5 trade easterlies and mid-latitude westerlies during the winter season. Rodwell and Hoskins  
6 (2001; hereafter RH01) argued that the monsoon heating generates a Kelvin wave response over  
7 the ocean to the east forming the equatorward portion of the subtropical anticyclone with a  
8 poleward low-level jet to satisfy Sverdrup balance. The heating also generates a Rossby wave  
9 response that produces adiabatic descent over regions to the west (Rodwell and Hoskins 1996).  
10 An equatorward low-level jet forms to satisfy Sverdrup balance closing off the subtropical  
11 anticyclone on its eastern flank. Additional effects, such as intense near-surface sensible heating  
12 over continents and air-sea interactions involving cold sea surface temperatures (SSTs) and low-  
13 level clouds in the eastern part of the oceans, also contribute to drive the subtropical anticyclones  
14 in the summer season (e.g., Seager et al. 2003; Liu et al. 2004; Miyasaka and Nakamura 2005).  
15 In the winter season, monsoon heating is absent and the subtropical anticyclones weaken.  
16 Consistent with this line of reasoning, the subtropical anticyclones in the Northern Hemisphere  
17 (NH) are stronger and better defined in the boreal summer than in winter (see Fig. 1 obtained  
18 with data from the NCEP-NCAR reanalysis). See Ting (1994), Chen et al. (2001) and Chen  
19 (2003) for further discussions on the stationary wave response to summer monsoon heating in the  
20 NH.

21 The subtropical anticyclones in the Southern Hemisphere (SH) behave in a qualitatively  
22 different manner: They are notably stronger in the austral winter than in summer over the  
23 Atlantic and Indian Oceans (see Fig. 1). This could be due to a combination of monsoons being

1 less important generators of zonal asymmetries in the mostly ocean-covered SH, and of  
2 topographic effects becoming stronger in winter as the flow intensifies. The former is plausible  
3 because the summertime subtropical anticyclones are significantly stronger in the NH than in the  
4 SH (Miyasaka and Nakamura 2010). However, an argument based on the seasonality of the SH  
5 is questionable because the SH has weaker seasonal variability. Furthermore, although the Andes  
6 cordillera is high and has strong slopes, the topography over southern Africa and Australia is  
7 relatively low and has a weaker blocking effect on the mean westerly flow (Richter and Mechoso  
8 2004; 2006).

9       Some revision of the RH01 conceptual model is, therefore, needed to address the seasonality  
10 of the southern subtropical anticyclones. Recent studies with numerical models have provided  
11 some guidance for such a revision. Wang et al. (2010) used an atmospheric general circulation  
12 model (AGCM) to demonstrate that convection over the Western Hemisphere warm pool  
13 (WHWP) during the boreal summer (austral winter) can produce adiabatic subsidence over the  
14 southeastern tropical Pacific, and thus contribute to maintaining the equatorward portion of the  
15 South Pacific subtropical anticyclone and the equatorward low-level jet along the South  
16 American coast. In addition, Wang et al. (2010) showed, by performing experiments with the  
17 simple two-level atmospheric model developed by Lee et al. (2009), that the interhemispheric  
18 connection between the WHWP and the South Pacific subtropical anticyclone depends critically  
19 on the configuration of the mean zonal winds in the SH. Richter et al. (2008) demonstrated a  
20 similar interhemispheric connection between the African - Indian summer monsoon and the  
21 South Atlantic subtropical anticyclone by comparing simulations by two versions of the  
22 University of California, Los Angeles (UCLA) AGCM that reproduce climate features with  
23 significantly different success.

1        On the basis of the studies by Wang et al. (2010) and Richter et al. (2008) one could advance  
2 the following conjecture. *Interhemispheric teleconnections associated with the major summer*  
3 *monsoons and deep tropical convection over warm SSTs in the NH contribute to the wintertime*  
4 *strengthening of the southern subtropical anticyclones.* The present study examines this  
5 conjecture. Our goals are to explore to what extent the southern subtropical anticyclones during  
6 the austral winter are affected by the major monsoons and deep tropical convection in the NH  
7 and to gain insight on the underlying mechanisms at work for the teleconnections. To achieve  
8 these goals we perform and analyze a suite of specially designed AGCM simulations  
9 complemented by additional experiments using a simple atmosphere model.

10        In evaluating the SH subtropical anticyclone response to NH convection, we focus primarily  
11 on sea level pressure (SLP). SLP will have contributions arising from both baroclinic and  
12 barotropic dynamics, and can be made precise in models that carry out a vertical mode  
13 decomposition (e.g., Lee et al. 2009; Neelin and Zeng 2000). In these, the first baroclinic mode  
14 has high surface pressure and cool tropospheric temperature in regions of upper-level  
15 convergence and adiabatic subsidence, and low surface pressure and warm tropospheric  
16 temperature in regions of diabatic heating. The baroclinic Rossby wave response to monsoon  
17 heating is at the core of the RH01 conceptual model, but can in turn excite barotropic Rossby  
18 waves via several interaction mechanisms: vertical wind shear and surface stress acting on the  
19 baroclinic mode, and vertical advection of baroclinic mode vorticity (e.g., Lee et al. 2009; Ji et  
20 al. 2013). The barotropic mode contribution to subtropical SLP can thus have significantly  
21 different teleconnection characteristics than the direct baroclinic mode contribution.

22        In section 2 we present our research strategy, give a brief description of the AGCM we use,  
23 and list the AGCM simulations we performed. Next, using the AGCM results, we describe the

1 SLP response in the SH over each ocean basin to the major summer monsoons in the NH. In  
2 sections 4 and 5, we analyze the AGCM simulations. We then posit that the major summer  
3 monsoons in the NH force interhemispheric meridional overturning circulation, and the diabatic  
4 cooling over certain sinking regions forces stationary barotropic Rossby waves in the  
5 extratropical SH to enhance the southern subtropical anticyclones. In section 6, this hypothesis is  
6 supported by specially designed experiments with the simple two-level model of Lee et al.  
7 (2009). Section 7 provides a summary and discussion.

8

## 9 **2. Strategy, model, and experiments**

10 Our strategy in this study is based on performing AGCM runs in which a control simulation  
11 (CTRL) is compared to an idealized experiment with artificially weakened summer monsoons in  
12 the NH (SYNC). This weakening in SYNC is achieved by shifting both the insolation at the top  
13 of the atmosphere (TOA) and the SSTs and sea ice cover in the NH by one-half the seasonal  
14 cycle (6 months) i.e., by synchronizing the seasonal cycles in the model's external and boundary  
15 conditions across hemispheres (See Fig. 2). In SYNC, therefore, there is a global warm season in  
16 December-February (DJF) and a global cold season in June-July (JJA), which, in the calendar  
17 year, correspond to those in the SH.

18 We use the NCAR Community Atmospheric Model version 4 (CAM4). CAM4 is a global  
19 atmosphere-land model with prescribed SSTs and sea ice cover (Neale et al. 2012). The finite  
20 volume dynamic core has a horizontal resolution of  $2.5^\circ$  (zonal)  $\times$   $1.9^\circ$  (meridional) and 26  
21 hybrid sigma-pressure layers. AGCM runs are 20-years long, of which the first five years are  
22 discarded to minimize any possible transient spinup effects. The time mean of the remaining 15  
23 years is analyzed in the following sections.

1

### 2 **3. Results**

3       Figure 3 shows the mean SLP obtained in CTRL for DJF and JJA. The simulated subtropical  
4 anticyclones are realistic, but are generally stronger than in the NCEP-NCAR reanalysis (see Fig.  
5 1). The simulation captures two important features of the subtropical anticyclones: 1) those in the  
6 NH are better defined in the boreal summer than in winter, and 2) those in the SH remain quite  
7 strong and well defined in the austral winter. In view of these results, it is reasonable to conclude  
8 that CAM4 is an appropriate tool for the present study.

9       Figure 4 shows time-latitude plots of monthly-mean, zonally averaged SLP over the South  
10 Pacific, South Atlantic and South Indian Oceans from the NCEP-NCAR reanalysis, CTRL and  
11 SYNC. The zonal average is carried out from the eastern to the western boundaries of the  
12 respective ocean basin.

13       Starting with the South Pacific, the maximum SLPs in both the NCEP-NCAR reanalysis and  
14 CTRL occurs during the austral spring (August-November; Figs. 4a and d). In SYNC, however,  
15 when the interhemispheric effect is removed, (Fig. 4g), the maximum SLPs occur in DJF and the  
16 minimum in July - August. This latter feature of the seasonal cycle is consistent with the  
17 monsoon heating mechanism of RH01. This suggests that the NH heating is a key contributor to  
18 the strength of the subtropical anticyclone over the South Pacific during the austral winter.

19       For the South Atlantic and South Indian Oceans, the maximum SLPs in both the NCEP-  
20 NCAR reanalysis and CTRL occurs around July - August (Figs. 4b and e). In SYNC (Fig. 4h),  
21 the maximum SLP occurs a little earlier with a much weaker magnitude than in CTRL (Fig. 4e).  
22 This suggests again that the NH heating plays a major role in the strengthened subtropical  
23 anticyclones over the South Atlantic and South Indian Oceans during the austral winter. It is

1 interesting to note that the maximum SLPs still does not occur in the austral summer, suggesting  
2 that the subtropical anticyclones over the South Atlantic and South Indian Oceans could be still  
3 strengthened during the austral winter without the NH heating. A potential mechanism that may  
4 explain this seasonal cycle in SYNC is discussed in section 7.

5 In summary, the AGCM experiments indicate that the interhemispheric response to the NH  
6 heating plays a crucial role in either maintaining or strengthening the southern subtropical  
7 anticyclones in the austral winter. The interhemispheric response is very strong over all three  
8 oceans, but it is more dramatic in the South Pacific, where the subtropical anticyclone nearly  
9 disappears in the austral winter without the influence from the NH. In the following sections we  
10 explore the physical processes that determine the interhemispheric response to the heating in the  
11 NH and its impact on the southern subtropical anticyclones.

12

#### 13 **4. Interhemispheric meridional overturning circulation**

14 In CTRL, the mean Hadley circulation during JJA (Fig. 5a) shows rising motion in the  
15 tropical NH and sinking motion in the tropical SH. In SYNC, with external and boundary  
16 forcings in the NH corresponding to DJF, this configuration changes drastically (Fig. 5b).  
17 Instead, there is a pair of “Hadley cells” with rising motion near the thermal equator at around  
18 5°N and sinking motion in the latitude band between 15° and 30° of each hemisphere. The  
19 difference in the Hadley circulations between CTRL and SYNC (Fig. 5c) is the net meridional  
20 overturning circulation forced by the NH heating during the warm season of that hemisphere.  
21 The net interhemispheric meridional overturning circulation shown in Fig. 5c is, in general,  
22 consistent with the suggestion on the association between the seasonal cycle of the Hadley cell  
23 and the monsoons put forward by Dima and Wallace (2003).



1 Associated with the net interhemispheric meridional overturning circulation (Fig. 5c) is the  
2 upper-level convergence field over the tropical SH. At the convergence centers subsiding air  
3 tends to yield local SLP increases (e.g., Rodwell and Hoskins 1996). It is important to point out,  
4 however, that the extent of the sinking branch of the net interhemispheric meridional overturning  
5 circulation is limited to the deep tropics equatorward of around 20°S (Fig. 5c). Therefore, the  
6 strengthening of the southern subtropical anticyclones south of around 20°S cannot be simply  
7 explained as the direct result of the net interhemispheric meridional overturning circulation  
8 forced from the NH.

9 Figure 6 shows the mean velocity potential and divergent winds during JJA at 200 hPa for  
10 CTRL, SYNC and CTRL - SYNC. In CTRL, divergent winds (rising motions) occur over India  
11 and East Asia, in association with the local summer monsoon, the northwestern tropical Pacific,  
12 and the WHWP, whereas convergent winds (sinking motions) occur over the southeastern  
13 tropical Pacific and much of the Atlantic especially the tropical South Atlantic (Fig. 6a). When  
14 the interhemispheric effect is removed (i.e. SYNC), the centers of rising motion in the NH are  
15 shifted toward the equator over the western equatorial Atlantic Ocean and the equatorial Indian  
16 Ocean (Fig. 6b). Therefore, the net result of the interhemispheric response to the heating in the  
17 NH is to produce subsidence over the western equatorial Atlantic Ocean and the equatorial  
18 Indian Ocean (Fig. 6c).

19 In addition, a broad region of subsidence exists in CTRL – SYNC over the south-central  
20 tropical Pacific, the southeastern tropical Pacific, and the tropical South Atlantic. It appears that  
21 the subsidence in the south-central tropical Pacific is linked mainly to the summer expansion of  
22 the western Pacific warm pool in the region of the northwestern tropical Pacific. The subsidence  
23 in the southeastern tropical Pacific appears to be linked to the WHWP consistent with Wang et

1 al. (2010), whereas the subsidence over the tropical South Atlantic appears to be linked to the  
2 Indian and West African summer monsoons, as suggested by Richter et al. (2008), and also to  
3 the WHWP. These effects occur essentially as baroclinic mode teleconnections, which have no  
4 trouble crossing the equator, but tend to remain trapped within the equatorial wave guide (Gill  
5 1980). In the next two sections, we turn to potential barotropic contributions.

6

## 7 **5. Propagation of stationary Rossby waves to the subtropics**

8 As shown in Fig. 7a, the interhemispheric effect on SLP is not limited to the tropical SH  
9 where the sinking branch of the net interhemispheric meridional overturning circulation directly  
10 increases the local SLPs. Over the regions of subsidence in the equatorial oceans and the tropical  
11 SH, slowly sinking air is heated by adiabatic compression and thus limits the vertical  
12 development of convection. Therefore, the sinking regions in the south-central Pacific Ocean, the  
13 western equatorial Atlantic Ocean, and the equatorial Indian Ocean are characterized by  
14 suppressed moist convective heating rate at 500 hPa (Figure 8) and reduced convective  
15 precipitation rate (not shown). Potentially, the diabatic cooling (i.e., reduced diabatic heating  
16 relative to SYNC) over these regions can produce stationary barotropic Rossby waves far beyond  
17 the tropics (e.g., Hoskins and Karoly 1981; Horel and Wallace 1981; Branstator 1983;  
18 Sardeshmukh and Hoskins 1988; Ting and Held 1990; Lee et al. 2009). Consistent with this  
19 hypothesis, the spatial pattern of SLPs in response to the interhemispheric teleconnections  
20 closely resembles the stream function response at 500 hPa, which is a widely used proxy to  
21 identify stationary barotropic Rossby waves (Fig. 7b). Note that the stream function sign is  
22 reversed (i.e., circulation is anticlockwise around positive stream function) for a better visual  
23 comparison with the SLP (Fig. 7a). It is important to point out that, due to cold SSTs and low

1 level clouds, conditions are not suitable for deep convection in the southeastern tropical Pacific  
2 or the southeastern tropical Atlantic. Therefore, the subsidence in these regions directly increases  
3 the SLPs locally, but cannot induce diabatic cooling (Fig. 8) or force stationary barotropic  
4 Rossby waves to the extratropical SH.

5

## 6 **6. Simple model experiments**

7 We next qualitatively examine the interpretation we have given to the differences between  
8 CTRL and SYNC, particularly to the forcing of stationary barotropic Rossby waves shown in  
9 Fig. 7b by diabatic cooling (i.e., reduced diabatic heating relative to SYNC) in the equatorial  
10 oceans and the tropical SH. For such examination we select the simple atmospheric model of Lee  
11 et al. (2009). This is a two-level, minimal complexity model of both the local and remote  
12 stationary responses of the atmosphere to tropical heating anomalies. The model equations are  
13 linearized about background wind fields, and recast as baroclinic and barotropic components  
14 with thermal advection in the tropics neglected. See Lee et al. (2009) and Wang et al. (2010) for  
15 more details about this model.

16 The band of easterlies in the tropics makes it difficult for stationary Rossby waves to  
17 propagate across the equator (e.g., Branstator 1983). This is particularly true if the stationary  
18 barotropic Rossby waves are forced in the tropical NH during the boreal summer when the zonal  
19 background barotropic flow is mainly westward equatorward of around 20°N (Pexoto and Oort  
20 1992). In the simple model experiments of Wang et al (2010), however, diabatic heating in the  
21 tropical NH directly influences the SH without invoking the associated diabatic cooling. In Wang  
22 et al. (2010), the baroclinic response to diabatic heating in the tropical NH comprises two centers  
23 of low SLP anomalies, one in the northwest and the other in the southwest of the forcing region,

1 consistent with the simple Gill model (Matsuno 1966; Gill 1980). As further investigated by Ji et  
2 al. (2013), the low SLP anomaly southwest of the forcing region in the tropical NH can be  
3 positioned in the tropical SH with a weaker amplitude compared to its counterpart in the NH.  
4 Also according to Ji et al. (2013), the Gill-type baroclinic circulations in the tropical SH may in  
5 turn interact with the background flows in this hemisphere to produce stationary barotropic  
6 Rossby waves.

7       Additionally, Watterson and Schneider (1987) suggested that a meridional background wind  
8 associated with the Hadley circulation could enable wave propagation across the equator even  
9 under an easterly background wind. Dima et al. (2005) analyzed the NCEP-NCAR reanalysis to  
10 find some supporting evidences. Kraucunas and Hartmann (2007), and Liu and Wang (2013)  
11 further demonstrated this mechanism using a nonlinear shallow-water model, and a linearized  
12 simple two-level model, respectively.

13       An important implication drawn from the above-mentioned studies is that summertime  
14 diabatic heating in the tropical NH can directly force stationary barotropic Rossby waves in the  
15 extratropical SH, without invoking the associated diabatic cooling in the equatorial oceans and  
16 the tropical SH, and thus can directly affect the southern subtropical anticyclones. Therefore, it is  
17 important to address how effectively the diabatic heating in the tropical NH can directly induce  
18 stationary barotropic Rossby waves in the extratropical SH.

19       In order to address these issues and also to further explore how the heating in the tropical NH  
20 and the cooling in the equatorial oceans and the tropical SH considered separately in six major  
21 forcing regions (see Fig. 8) affect the southern subtropical anticyclones, we performed seven  
22 experiments using the two-level model. In the first experiment, the moist convective heating rate  
23 at 500 hPa for JJA obtained from CTRL – SYNC (Fig. 8) is prescribed. The other six

1 experiments are identical to the first, except that the thermal forcing is prescribed only over  
2 selected regions (see Fig. 8). In the second, third and fourth experiments, the moist convective  
3 heating rate is prescribed only in the south-central Pacific ( $150^{\circ}\text{E} - 130^{\circ}\text{W}$  and  $20^{\circ}\text{S} - 5^{\circ}\text{N}$ ), the  
4 western equatorial Atlantic ( $60^{\circ}\text{W} - 10^{\circ}\text{W}$  and  $10^{\circ}\text{S} - 7.5^{\circ}\text{N}$ ), and the equatorial Indian Ocean  
5 ( $60^{\circ}\text{E} - 110^{\circ}\text{W}$  and  $20^{\circ}\text{S} - 10^{\circ}\text{N}$ ), respectively. In the fourth, fifth and sixth experiments, the  
6 moist convective heating rate is prescribed only in the northwestern Pacific Ocean affected by  
7 summer expansion of the western Pacific warm pool ( $110^{\circ}\text{E} - 160^{\circ}\text{W}$  and  $5^{\circ}\text{N} - 30^{\circ}\text{N}$ ), the  
8 WHWP ( $100^{\circ}\text{W} - 60^{\circ}\text{W}$  and  $5^{\circ}\text{N} - 20^{\circ}\text{N}$ ), and the Indian summer monsoon region ( $20^{\circ}\text{W} -$   
9  $110^{\circ}\text{E}$  and  $10^{\circ}\text{N} - 30^{\circ}\text{N}$ ), respectively. See Fig. 8 for the regions of forcing and the heating rates  
10 prescribed for these experiments.

11 For all seven experiments, the background fields are the zonally averaged climatological  
12 stream function and velocity potential for JJA in the upper and lower troposphere derived from  
13 CTRL. The simple two-level model assumes that barotropic divergence is zero (Lee et al. 2009).  
14 Thus, the model is prescribed with only the baroclinic background velocity potential, which is  
15 directly related to the Hadley cell in CTRL (Fig. 5a), and with both the barotropic and baroclinic  
16 background stream functions. The zonally averaged barotropic and baroclinic background zonal  
17 winds and the zonally averaged baroclinic meridional winds (computed from the stream function  
18 and velocity potential fields) derived from SYNC and CTRL are shown in Fig. 9 along with  
19 those derived from the NCEP-NCAR reanalysis. Since the simple model mainly solves a set of  
20 linearized equations, nonlinear effects are not considered in our experiments.

21 Figure 10 shows the barotropic stream function response to the thermal forcing shown in Fig.  
22 8. The stream function sign is again reversed (i.e., circulation is anticlockwise around positive  
23 stream function) for a better visual comparison with the SLP in the AGCM experiments (Fig.

1 7a). The simple two-level model is an oversimplification of the real atmosphere, and is unable to  
2 reproduce the exact shape or propagation pathway of the stationary Rossby waves simulated by  
3 CAM4 (Fig. 7b). Nevertheless, a comparison between Figs. 7b and 10 reveals several important  
4 common features. In particular, the anticyclones are roughly in place to enhance the southern  
5 subtropical anticyclones in all three oceans.

6 Figure 11a, b and c show the barotropic stream function response to diabatic cooling in the  
7 south-central Pacific Ocean, the western equatorial Atlantic Ocean, and the equatorial Indian  
8 Ocean, respectively. It is clear that the stationary barotropic Rossby waves originating from the  
9 south-central Pacific greatly strengthen the South Pacific subtropical anticyclone. Similarly, the  
10 stationary barotropic Rossby waves originating from the western equatorial Atlantic Ocean  
11 propagate to the extratropical South Atlantic and strengthen the South Atlantic subtropical  
12 anticyclone. It appears that diabatic cooling in the equatorial Indian Ocean and the associated  
13 stationary waves contribute to the strength of the South Indian subtropical anticyclone  
14 particularly to the south and west of Australia.

15 Figure 12a, b and c show the barotropic stream function response to diabatic heating in the  
16 northwestern Pacific Ocean, the WHWP, and the Indian summer monsoon region, respectively.  
17 Unlike those forced in the south-central Pacific Ocean, the stationary barotropic Rossby waves  
18 forced in the northwestern Pacific Ocean hardly influence the southern subtropical anticyclones.  
19 The stationary waves directly forced in the WHWP only weakly influence the South Pacific  
20 subtropical anticyclone.

21 However, it is interesting to note that the stationary waves directly forced in the Indian  
22 summer monsoon region have large influences on the South Pacific and South Atlantic  
23 subtropical anticyclones. This experiment is repeated without the baroclinic background

1 meridional winds to find that the baroclinic background meridional winds across the equator  
2 (i.e., interhemispheric overturning circulation) play an important role in enhancing the  
3 propagation of the Indian summer monsoon-forced stationary waves to the SH, in line with the  
4 explanation offered by Watterson and Schneider (1987).

5 In summary, the simple model experiments support our hypothesis that, in response to the  
6 heating in the tropical NH, diabatic cooling occurs in the equatorial oceans and the tropical SH,  
7 and the cooling in the equatorial oceans and the tropical SH in turn force the stationary  
8 barotropic Rossby waves shown in Fig. 7b, and thus strengthens the southern subtropical  
9 anticyclones. The simple model experiments suggest that diabatic heating in the Indian summer  
10 monsoon region can also enhance the South Pacific and South Atlantic subtropical anticyclones  
11 without invoking the cooling in the equatorial oceans and the tropical SH.

12 In interpreting these barotropic Rossby wave trains, it should be recalled that they are excited  
13 in the simple model by the prescribed diabatic heating or cooling (see Lee et al. 2009). The  
14 diabatic cooling is itself a teleconnected response to heating in the tropical NH and is primarily a  
15 reduction in deep convective heating that could potentially occur in certain locations over the  
16 equatorial oceans and the tropical SH if the tropical NH heating were absent. It is also important  
17 to recall that the simple two-level model does not include moist processes. Therefore, unless  
18 prescribed, the simple model cannot simulate diabatic processes such as radiative cooling or  
19 convective heating. See an intermediate complexity model study by Ji et al. (2013) for further  
20 discussions on interhemispheric teleconnections in response to a localized heat source in the  
21 tropical NH via the baroclinic mode affecting moist processes and thus convective heating in the  
22 tropical SH.

23

## 1 **7. Summary and discussions**

2 The present study examines the conjecture that major summer monsoons in the NH  
3 contribute to the wintertime strengthening of the southern subtropical anticyclones through  
4 interhemispheric teleconnections. To explore this conjecture, we perform a specially designed  
5 suite of AGCM experiments in which summer monsoons in the NH are artificially weakened. To  
6 elucidate the underlying mechanisms at work for the teleconnections we also perform several  
7 experiments using the simple numerical two-level model of Lee et al. (2009).

8 The results obtained in the AGCM and simple model experiments suggest that the  
9 interhemispheric response to the heating in the NH does play a crucial role in either maintaining  
10 or strengthening the southern subtropical anticyclones in the austral winter. Although the  
11 interhemispheric response is very strong over all three oceans, it is more dramatic in the South  
12 Pacific since subtropical anticyclone over this ocean nearly disappears in the austral winter  
13 without the influence from the NH.

14 The sketch in Figure 13 encapsulates results from several parts in the text. During the boreal  
15 summer, the interhemispheric meridional overturning circulation is fueled from three hot spots in  
16 the tropical NH. These spots are located over the Indian - East Asian summer monsoon region,  
17 the northwestern tropical Pacific region affected by summer expansion of the western Pacific  
18 warm pool, and the WHWP (see Fig. 6). The associated subsidence and SLP increases occur  
19 over the western equatorial Atlantic Ocean, the equatorial Indian Ocean, the south-central  
20 tropical Pacific Ocean, the southeastern tropical Pacific Ocean, and the South Atlantic Ocean.  
21 Since conditions are suitable for deep convection in the western equatorial Atlantic Ocean, the  
22 equatorial Indian Ocean, and the south-central tropical Pacific Ocean due to warm SSTs therein,  
23 the subsidence over these three regions suppresses convection (see Fig. 8). The diabatic cooling



1 (i.e., reduced diabatic heating relative to SYNC) in these regions produces stationary barotropic  
2 Rossby waves that propagate far beyond the tropical SH. These stationary Rossby waves and  
3 those forced directly by the summer heating in the tropical NH are spatially phased to strengthen  
4 the southern subtropical anticyclones over all three oceans.

5 It is argued that the stationary barotropic Rossby waves forced directly by heating in the  
6 tropical NH have a generally weaker influence on the southern subtropical anticyclones than  
7 those forced by cooling in the equatorial oceans and the tropical SH. However, the simple two-  
8 level model used to arrive at that conclusion excludes nonlinear effects. Therefore, further  
9 analyses are needed to clarify this point. A potentially promising method is to prescribe localized  
10 heating profiles in a fully nonlinear AGCM (e.g., Jang and Strauss, 2012).

11 The subtropical anticyclones over the South Atlantic and South Indian Oceans could be still  
12 strengthened during the austral winter without the NH convective heating (Fig. 4h and i). It  
13 appears that in the absence of the NH heating the equatorial oceans, especially the equatorial  
14 Indian Ocean, could drive rising motions aloft to force subsidence motions over the broad  
15 regions of South Atlantic and southwestern Indian Ocean (see Fig. 6b), and thus increase SLPs  
16 therein.

17 The results of this study leave open some important scientific questions, which deserve future  
18 investigations. For instance, in our AGCM experiments the model SSTs in the SH are not  
19 allowed to respond to (or to the lack of) the interhemispheric teleconnections. Therefore, it  
20 remains to be determined if and how our conclusions are modified if thermal and dynamic  
21 interactions with the surface ocean mixed layer are activated. An important and related point is  
22 that the trade winds over the SH are closely linked to the southern subtropical anticyclones. An  
23 enhanced southern subtropical anticyclone during the boreal summer could potentially increase

1 the trade winds in the SH, and thus affect surface ocean dynamics and SSTs in the tropical SH.  
2 To explore potential air-sea interactions involving the interhemispheric teleconnections, the next  
3 step is to perform experiments of the CTRL and SYNC type with CAM4 coupled to a slab ocean  
4 mixed layer model over the SH.

5  
6 **Acknowledgments.** We would like to thank three anonymous reviewers for their thoughtful  
7 comments and suggestions, which led to a significant improvement of the paper. We also would  
8 like to thank Teresa Losada, Xiao Heng, and Xuan Ji for their helpful comments and  
9 contributions through our science discussions between the University of Miami and UCLA, and  
10 Marlos Goes and George Halliwell for their useful comments and suggestions. This work was  
11 supported by grants from the National Science Foundation (NSF) and the National Oceanic and  
12 Atmospheric Administration (NOAA)'s Climate Program Office, and by the base funding of  
13 NOAA Atlantic Oceanographic and Meteorological Laboratory (AOML).

## 14 15 **REFERENCES**

- 16 Branstator, G., 1983: Horizontal energy propagation in a barotropic atmosphere with meridional  
17 and zonal structure. *J. Atmos. Sci.*, **40**, 1689–1708.
- 18 Chen, P., M. P. Hoerling, and R. M. Dole, 2001: The origin of the subtropical anticyclones. *J.*  
19 *Atmos. Sci.*, **58**, 1827–1835.
- 20 Chen, T.-C., 2003: Maintenance of summer monsoon circulations: A planetary-scale perspective.  
21 *J. Climate*, **16**, 2022–2037.
- 22 Dima, I. M., and J. M. Wallace, 2003: On the seasonality of the Hadley cell. *J. Atmos. Sci.*, **60**,  
23 1522-1527.

1 Dima, I. M., J. M. Wallace, I. Kraucunas, 2005: Tropical zonal momentum balance in the NCEP  
2 reanalyses. *J. Atmos. Sci.*, **62**, 2499-2513.

3 Gill, A. E., 1980: Some simple solutions for heat-induced tropical circulation. *Quart. J. Roy.*  
4 *Meteor. Soc.*, **106**, 447–462.

5 Horel, J. D., and J. M. Wallace, 1981: Planetary-scale atmospheric phenomena associated with  
6 the Southern Oscillation. *Mon. Wea. Rev.*, **109**, 813–829.

7 Hoskins, B. J., and D. J. Karoly, 1981: The steady linear response of a spherical atmosphere to  
8 thermal and orographic forcing. *J. Atmos. Sci.*, **38**, 1179–1196.

9 Jang, Y., D. M. Straus, 2012: The Indian monsoon circulation response to El Niño diabatic  
10 heating. *J. Climate*, **25**, 7487–7508.

11 Ji, X., J. D. Neelin, S.-K. Lee, and C. R. Mechoso, 2013: Interhemispheric teleconnections from  
12 tropical heat sources in intermediate and simple models. *J. Climate*, in-revision.

13 Kraucunas, I., and D. L. Hartmann, 2007: Tropical stationary waves in a nonlinear shallow-  
14 water model with realistic basic states. *J. Atmos. Sci.*, **64**, 2540-2557.

15 Lee, S.-K., C. Wang, and B. Mapes, 2009: A simple atmospheric model of the local and  
16 teleconnection responses to heating anomalies. *J. Climate*, **22**, 272-284.

17 Liu, F., and B. Wang, 2013: Mechanisms of global teleconnections associated with the Asian  
18 summer monsoon: An intermediate model analysis. *J. Climate*, **26**, 1791–1806.

19 Liu, Y. M., G. X. Wu, and R. Ren, 2004: Relationship between the subtropical anticyclone and  
20 diabatic heating. *J. Climate*, **17**, 682–698.

21 Matsuno, T., 1966: Quasi-geostrophic motions in the equatorial area. *J. Meteor. Soc. Japan*, **44**,  
22 25–43.

- 1 Miyasaka, T., and H. Nakamura, 2005: Structure and formation mechanisms of the Northern  
2 Hemisphere summertime subtropical highs. *J. Climate*, **18**, 5046–5065.
- 3 Miyasaka, T., and H. Nakamura, 2010: Structure and mechanisms of the Southern Hemisphere  
4 summertime subtropical anticyclones. *J. Climate*, **23**, 2115–2130.
- 5 Neale, R. B., J. Richter, S. Park, P. H. Lauritzen, S. J. Vavrus, P. J. Rasch, and M. Zhang, 2012:  
6 The mean climate of the community atmosphere model (CAM4) in forced SST and fully  
7 coupled experiments. *J. Climate*, submitted.
- 8 Neelin, J. D., and N. Zeng, 2000: A quasi-equilibrium tropical circulation model – formulation.  
9 *J. Atmos. Sci.*, **57**, 1741-1766.
- 10 Peixoto, J. P., and A. H. Oort, 1992: *Physics of Climate*. American Institute of Physics, 520 pp.
- 11 Richter, I., and C. R. Mechoso, 2004: Orographic influences on the annual cycle of Namibian  
12 stratocumulus clouds. *Geophys. Res. Lett.*, **31**, L24108.
- 13 Richter, I. and C. R. Mechoso, 2006: Orographic influences on subtropical stratocumulus. *J.*  
14 *Atmos. Sci.*, **63**, 2585-2601.
- 15 Richter, I., C. R. Mechoso, and A. W. Robertson, 2008: What determines the position and  
16 intensity of the South Atlantic anticyclone in austral winter? - An AGCM study. *J. Climate*,  
17 **21**, 214–229.
- 18 Rodwell, M. J., and B. J. Hoskins, 1996: Monsoons and the dynamics of deserts. *Q. J. Roy.*  
19 *Meteorol. Soc.*, **122**, 1385-1404.
- 20 Rodwell, M. J., and B. J. Hoskins, 2001: Subtropical anticyclones and summer monsoons. *J.*  
21 *Climate*, **14**, 3192-3211.
- 22 Sardeshmukh, P. D., and B. J. Hoskins, 1988: The generation of global rotational flow by steady  
23 idealized tropical divergence. *J. Atmos. Sci.*, **45**, 1228–1251.

1 Seager, R., R. Murtugudde, N. Naik, A. Clement, N. Gordon, and J. Miller, 2003: Air sea  
2 interaction and the seasonal cycle of the subtropical anticyclones. *J. Climate*, **16**, 1948-1966.

3 Ting, M., and I. M. Held, 1990: The stationary wave response to tropical SST anomaly in an  
4 idealized GCM. *J. Atmos. Sci.*, **47**, 2546–2566.

5 Ting, M., 1994: Maintenance of northern summer stationary waves in a GCM. *J. Atmos. Sci.*, **51**,  
6 3286–3308.

7 Wang, C., S.-K. Lee, and C. R. Mechoso, 2010: Interhemispheric influence of the Atlantic warm  
8 pool on the southeastern Pacific. *J. Climate*, **23**, 404-418.

9 Watterson, I. G., and E. K. Schneider, 1987: The effect of the Hadley Circulation on the  
10 meridional propagation of stationary waves. *Q. J. Roy. Meteor. Soc.*, **13**, 779–813.

11  
12  
13  
14  
15  
16  
17  
18  
19  
20  
21  
22  
23

1 **Figure captions:**

2

3 Figure 1. Mean sea level pressure for (a) DJF and (JJA) during 1971 – 2000 from the NCEP-  
4 NCAR Reanalysis. The unit is hPa.

5

6 Figure 2. Daily solar insolation at the top of the atmosphere in (a) CTRL, (b) SYNC, and (c)  
7 CTRL – SYNC. The unit is  $W m^{-2}$ .

8

9 Figure 3. Mean sea level pressure for (a) DJF and (b) JJA from CTRL. The unit is hPa.

10

11 Figure 4. Seasonal cycle of sea level pressure averaged zonally for (a, d, and g) the South Pacific  
12 Ocean, (b, e, and h) the South Atlantic Ocean, and (c, f, and i) South Indian Ocean from the  
13 NCEP-NCAR reanalysis (top row), CTRL (middle row), and SYNC (bottom row). The unit is  
14 hPa.

15

16 Figure 5. Mean meridional overturning circulation (mass stream function) obtained from (a)  
17 CTRL, (b) SYNC, and (c) CTRL – SYNC. Circulation is clockwise (anticlockwise) around  
18 positive (negative) stream function. The unit is  $10^9 Kg s^{-1}$ .

19

20 Figure 6. Mean velocity potential and divergent wind vector at 200 hPa from (a) CTRL, (b)  
21 SYNC, and (c) CTRL - SYNC. The units are  $10^7 m^2 s^{-1}$  for velocity potential, and  $m s^{-1}$  for  
22 divergent wind vector.

23

1 Figure 7. (a) Mean sea level pressure, (b) stream function and wind vector at 500 hPa from  
2 CTRL - SYNC. The zonal line at 40°S roughly marks the southern end of the southern  
3 subtropical anticyclones in JJA. The stream function sign is reversed in such a way that  
4 circulation is anticlockwise around positive stream function. The units are hPa for sea level  
5 pressure,  $10^7 \text{ m}^2 \text{ s}^{-1}$  for stream function, and  $\text{m s}^{-1}$  for wind vector.

6

7 Figure 8. Mean moist convective heating rate at 500 hPa for JJA from CTRL - SYNC. The unit  
8 is  $\text{K day}^{-1}$ . The three regions of diabatic heating in the NH, namely the northwestern Pacific  
9 Ocean affected by summer expansion of the western Pacific warm pool, the, and the Indian  
10 summer monsoon region are indicated by red borderlines. The three regions of diabatic cooling  
11 in the equatorial oceans and the tropical SH, namely the south-central Pacific, the western  
12 equatorial Atlantic, and the equatorial Indian Ocean are shown with blue borderlines.

13

14 Figure 9. Zonally averaged climatological (a) barotropic zonal, (b) baroclinic zonal and (c)  
15 baroclinic meridional winds in JJA obtained from SYNC (solid lines), CTRL (long-dashed lines)  
16 and the NCEP-NCAR reanalysis (short-dashed line). The barotropic zonal winds are obtained by  
17 vertically averaging the zonal winds in the troposphere (100 ~ 1000 hPa). To compute the  
18 baroclinic zonal winds, the zonal winds are vertically averaged separately for the upper  
19 troposphere (100 ~ 500 hPa) and for the lower troposphere (500 ~ 1000 hPa), and the latter is  
20 subtracted from the former then divided by 2. The same methodology is used to compute the  
21 baroclinic meridional winds.

22

1 Figure 10. Barotropic stream function and wind vector responses in the simple model  
2 experiments to the moist convective heating and cooling derived from CTRL – SYNC. The units  
3 are  $10^7 \text{ m}^2 \text{ s}^{-1}$  for stream function, and  $\text{m s}^{-1}$  for wind vector.

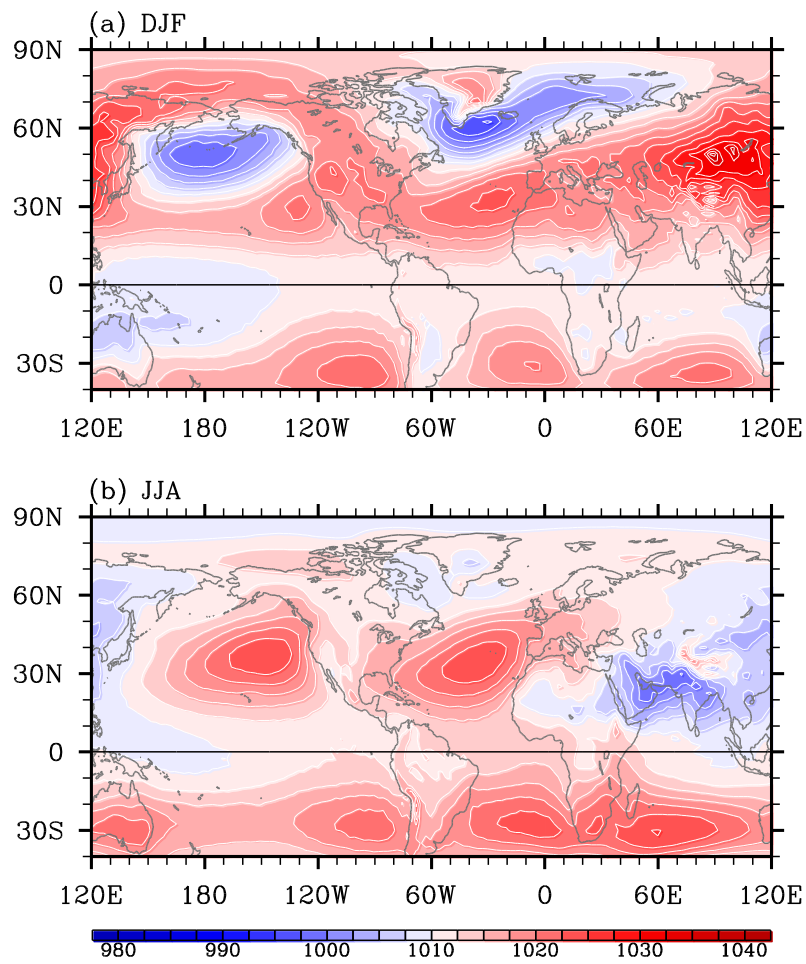
4  
5 Figure 11. Barotropic stream function and wind vector responses in the simple model  
6 experiments to diabatic cooling in (a) the central South Pacific Ocean, (b) the western equatorial  
7 Atlantic Ocean, and (c) the equatorial Indian Ocean. The units are  $10^7 \text{ m}^2 \text{ s}^{-1}$  for stream function,  
8 and  $\text{m s}^{-1}$  for wind vector.

9  
10 Figure 12. Barotropic stream function and wind vector responses in the simple model  
11 experiments to diabatic heating in (a) the northwestern Pacific Ocean, (b) the WHWP, and (c)  
12 the Indian summer monsoon region. The units are  $10^7 \text{ m}^2 \text{ s}^{-1}$  for stream function, and  $\text{m s}^{-1}$  for  
13 wind vector.

14  
15 Figure 13. Sketch of the physical processes linking the major summer monsoons in the NH and  
16 the southern subtropical anticyclones. The three regions of rising motion, the three regions of  
17 sinking motion and the regions of southern subtropical anticyclones affected are filled with gray,  
18 sky blue and red colors, respectively. The sinking regions in the southeastern tropical Pacific and  
19 the southeastern tropical Atlantic are indicated by sky blue borderlines. Thick black arrows  
20 represent divergent winds in the upper level, while light green arrows represent the ray paths of  
21 the stationary barotropic Rossby waves forced by diabatic cooling over the three regions of  
22 sinking motion and by diabatic heating in the Indian summer monsoon region.



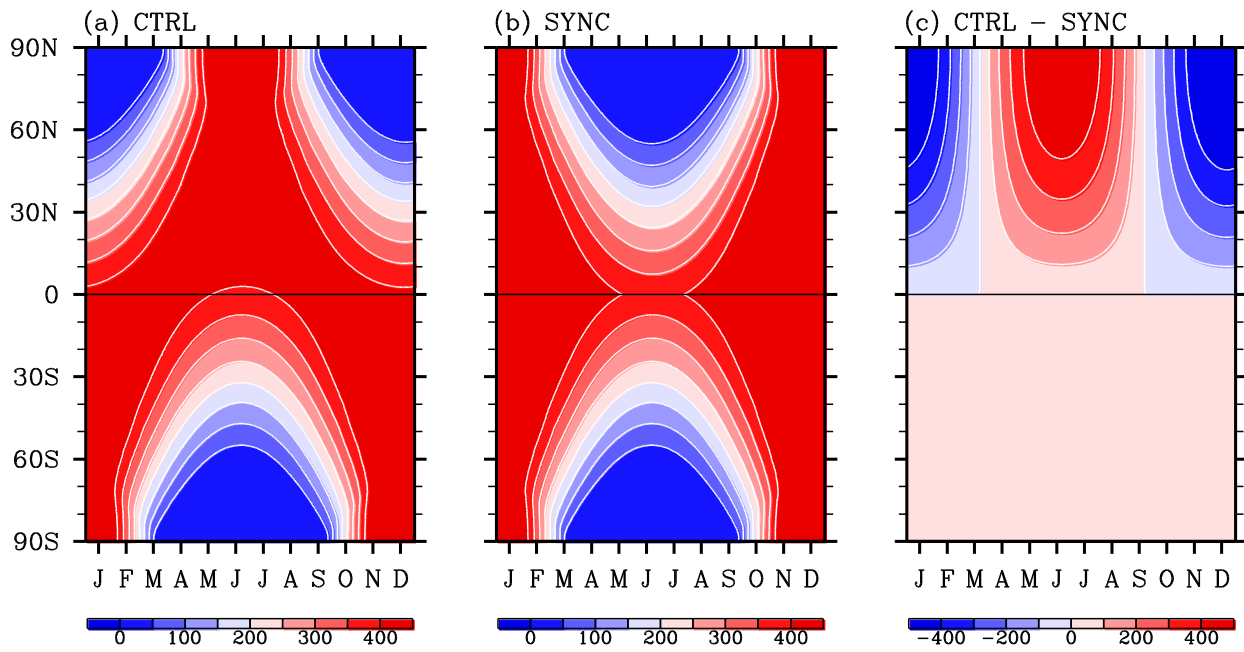
NCEP–NCAR Reanalysis: SLP



1  
 2 Figure 1. Mean sea level pressure for (a) DJF and (JJA) during 1971 - 2000 from the NCEP-  
 3 NCAR Reanalysis. The unit is hPa.

4  
 5  
 6  
 7  
 8  
 9  
 10  
 11  
 12  
 13

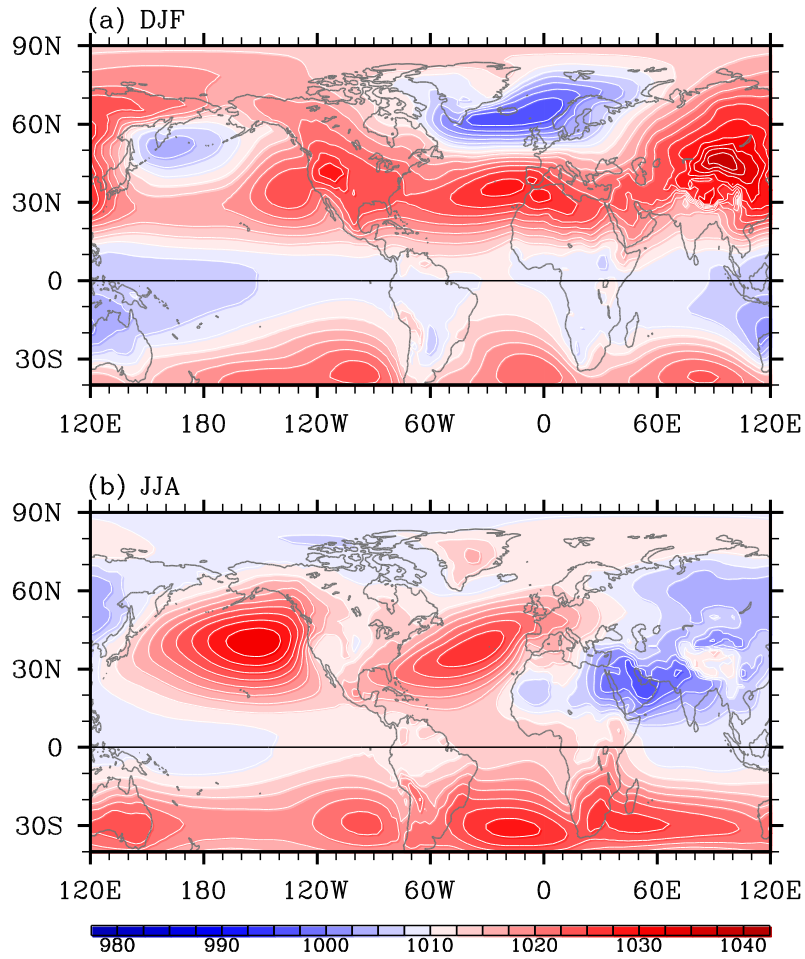
CAM4: TOA Solar Insolation



1  
2  
3  
4  
5  
6  
7  
8  
9  
10  
11  
12  
13  
14  
15  
16  
17  
18  
19

Figure 2. Daily solar insolation at the top of the atmosphere in (a) CTRL, (b) SYNC, and (c) CTRL - SYNC. The unit is  $\text{W m}^{-2}$ .

CAM4 (CTRL): SLP



1

2 Figure 3. Mean sea level pressure for (a) DJF and (b) JJA from CTRL. The unit is hPa.

3

4

5

6

7

8

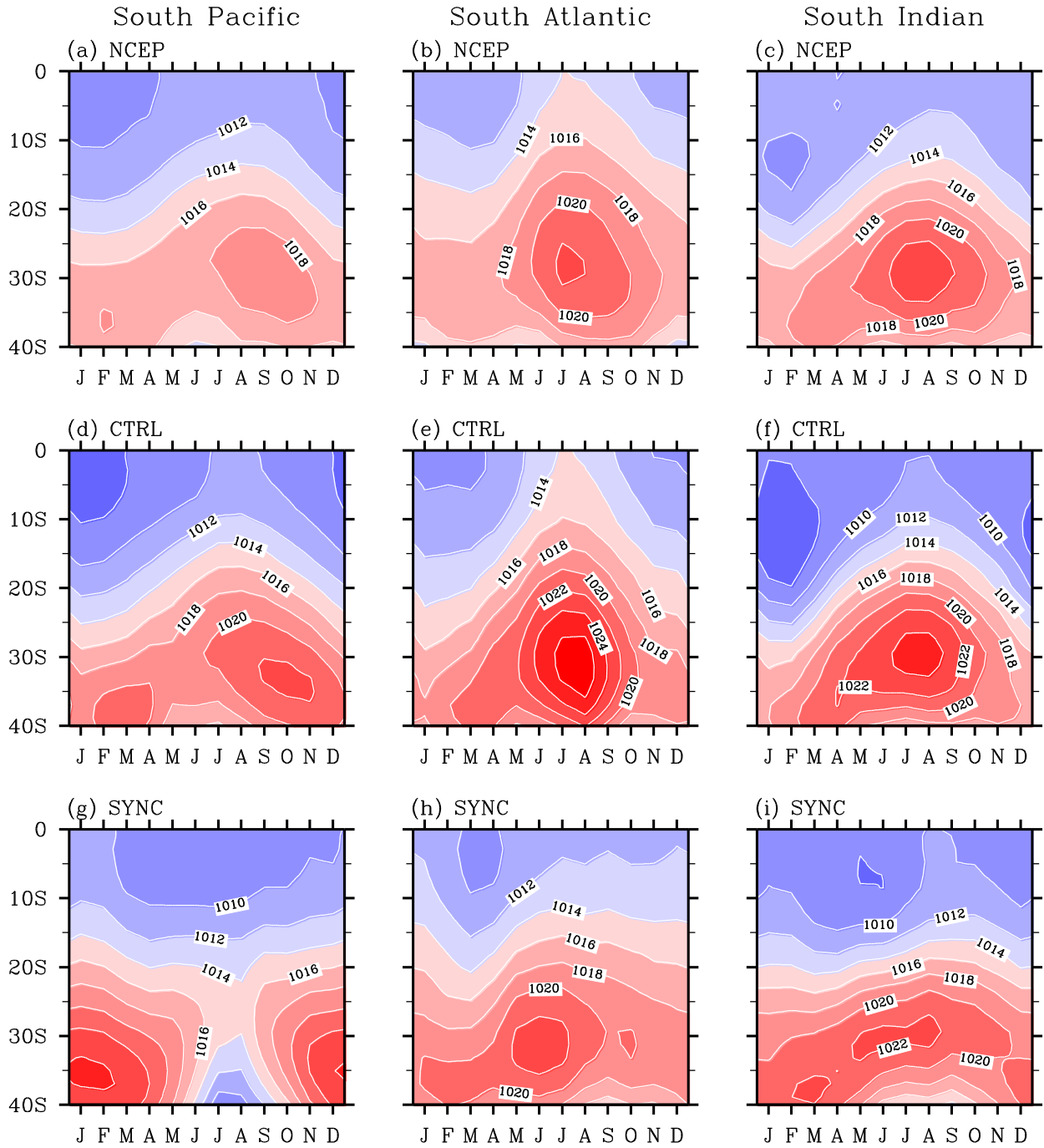
9

10

11

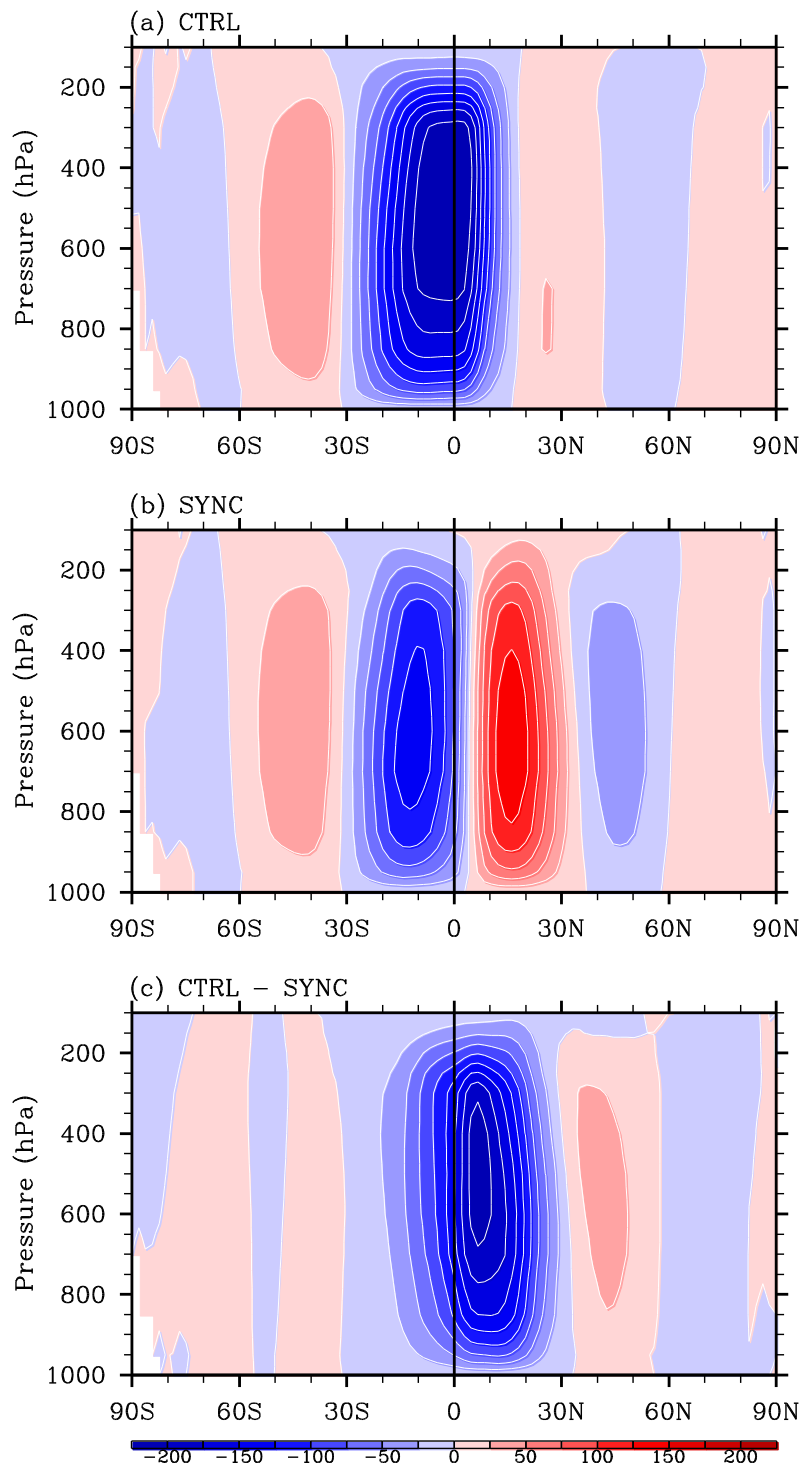
12

NCEP & CAM4: Zonally Averaged SLP for Each Ocean Basin



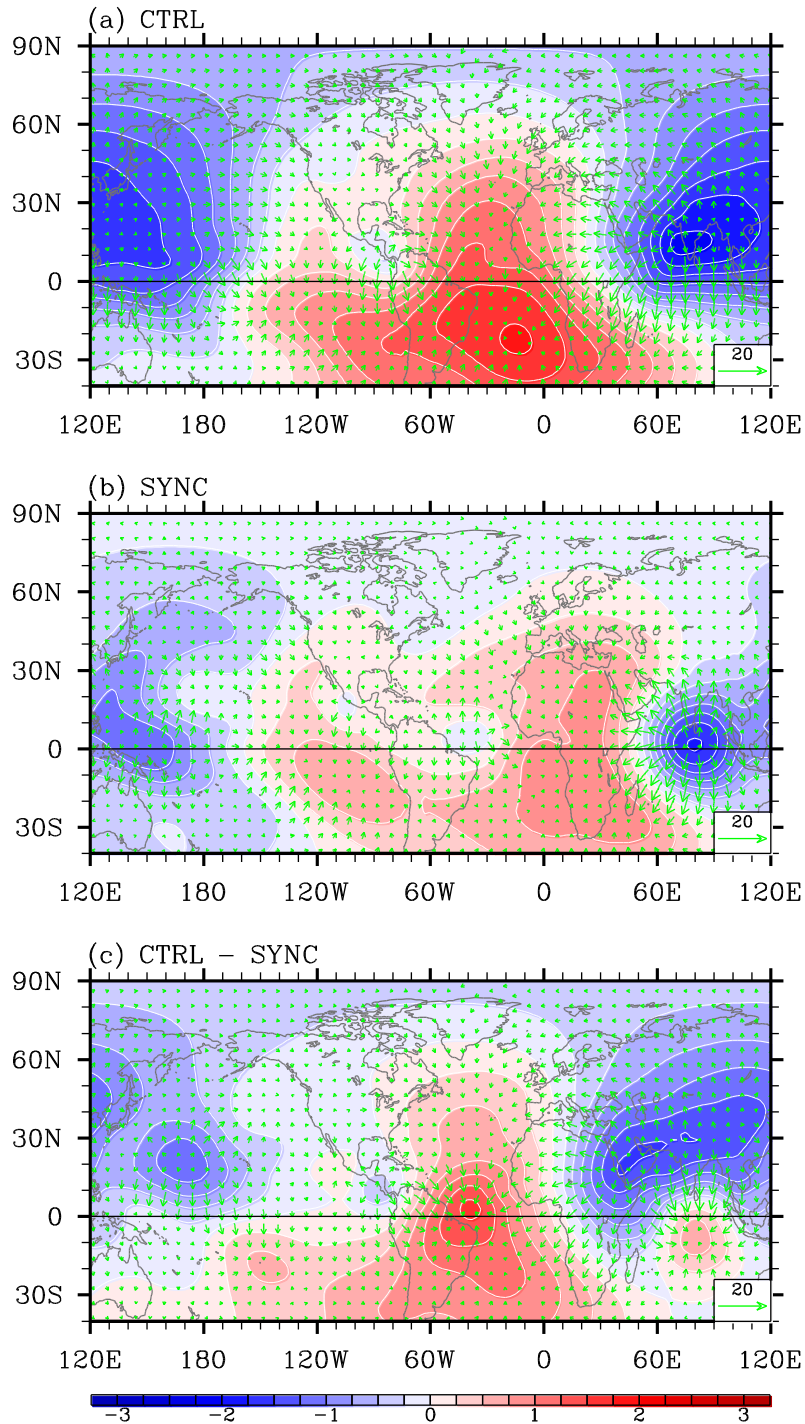
1  
 2 Figure 4. Seasonal cycle of sea level pressure averaged zonally for (a, d, and g) the South Pacific  
 3 Ocean, (b, e, and h) the South Atlantic Ocean, and (c, f, and i) South Indian Ocean from the  
 4 NCEP-NCAR reanalysis (top row), CTRL (middle row), and SYNC (bottom row). The unit is  
 5 hPa.

CAM4: Hadley Circulation (JJA)



1  
2 Figure 5. Mean meridional overturning circulation (mass stream function) from (a) CTRL, (b)  
3 SYNC, and (c) CTRL - SYNC. Circulation is clockwise (anticlockwise) around positive  
4 (negative) stream function. The unit is  $10^9 \text{ Kg s}^{-1}$ .

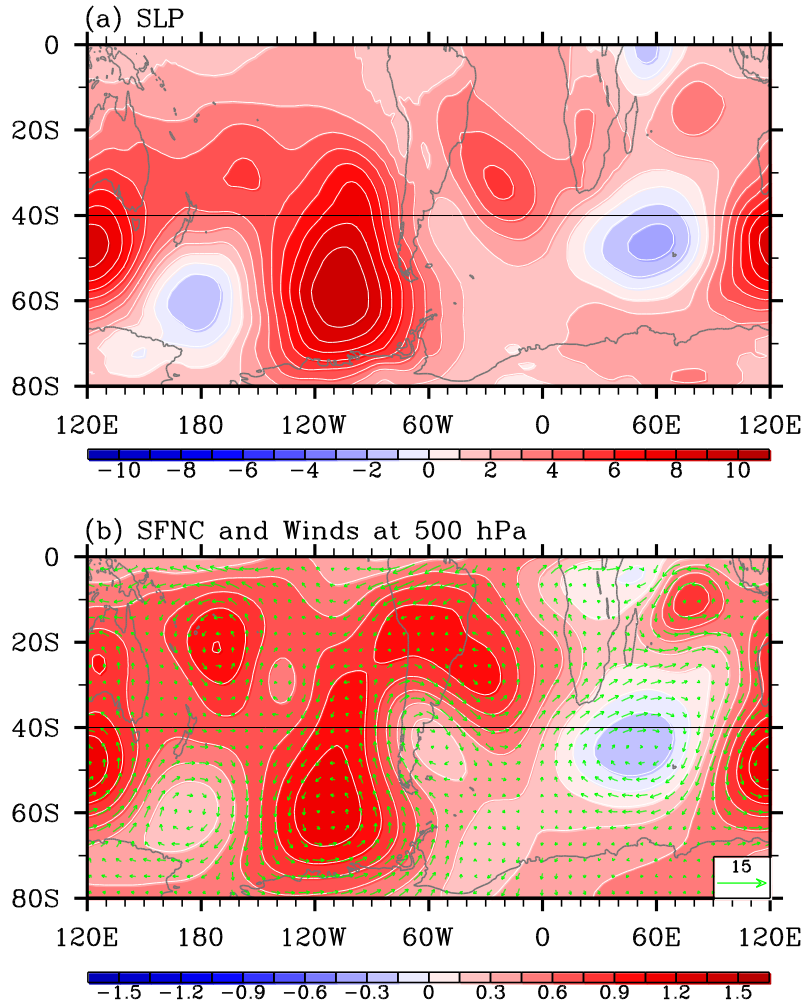
CAM4: VPOT & DIV Wind at 200hPa (JJA)



1  
2 Figure 6. Mean velocity potential and divergent wind vector at 200 hPa obtained from (a) CTRL,  
3 (b) SYNC, and (c) CTRL - SYNC. The units are  $10^7 \text{ m}^2 \text{ s}^{-1}$  for velocity potential, and  $\text{m s}^{-1}$  for  
4 divergent wind vector.

5

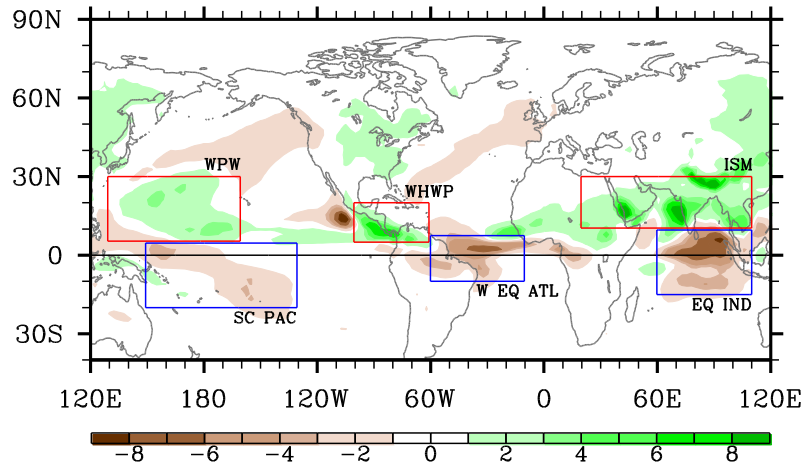
CAM4: CTRL - SYNC (JJA)



1  
2 Figure 7. (a) Mean sea level pressure, (b) stream function and wind vector at 500 hPa from  
3 CTRL - SYNC. The zonal line at 40°S roughly marks the southern end of the southern  
4 subtropical anticyclones in JJA. The stream function sign is reversed in such a way that  
5 circulation is anticlockwise around positive stream function. The units are hPa for sea level  
6 pressure, m for geopotential, and  $\text{m s}^{-1}$  for wind vector.

7  
8  
9  
10  
11  
12

CAM4 (CTRL - SYNC): Conv. Heating (JJA)

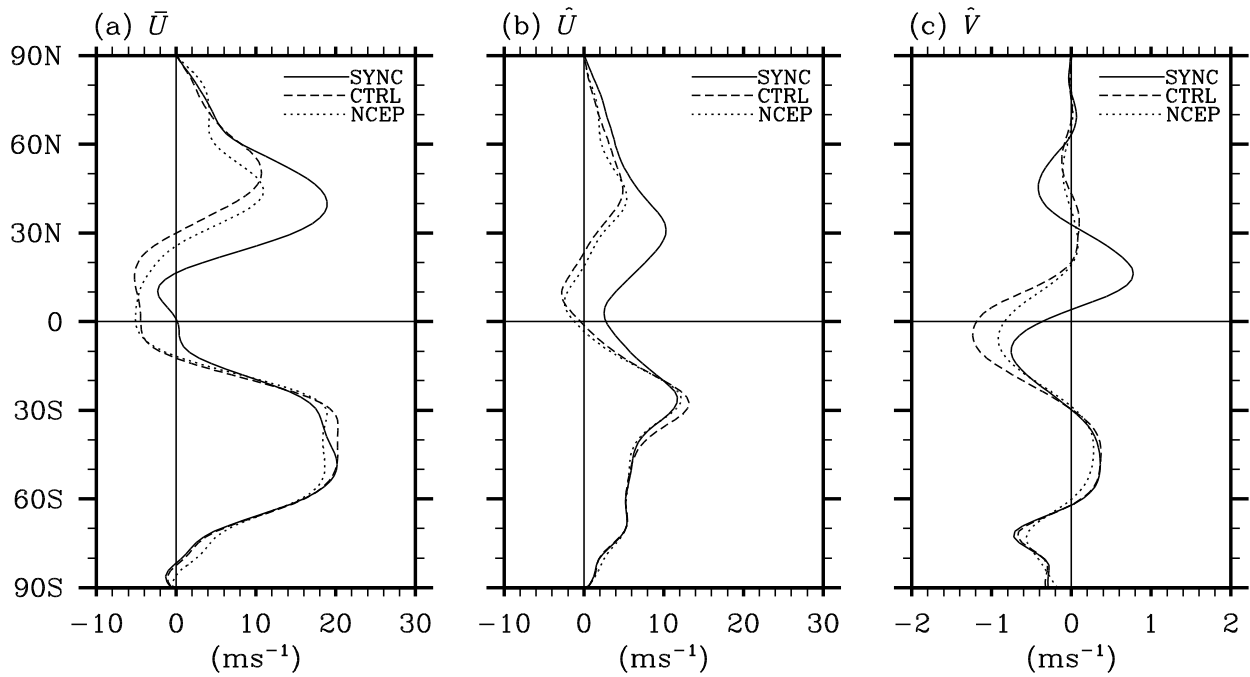


1  
2 Figure 8. Mean moist convective heating rate at 500 hPa for JJA from CTRL - SYNC. The three  
3 regions of diabatic heating in the NH, namely the northwestern Pacific Ocean affected by  
4 summer expansion of the western Pacific warm pool, the WHWP, and the Indian summer  
5 monsoon region are indicated by red borderlines. The three regions of diabatic cooling in the  
6 equatorial oceans and the tropical SH, namely the south-central Pacific, the western equatorial  
7 Atlantic, and the equatorial Indian Ocean are shown with blue borderlines. The unit is K day<sup>-1</sup>.

8  
9  
10  
11  
12  
13  
14  
15  
16  
17  
18  
19  
20



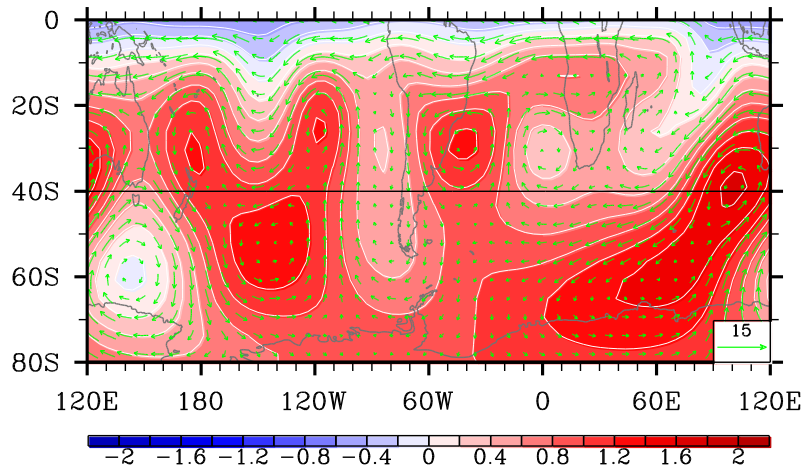
## NCEP & CAM4: Background Flow (JJA)



1  
 2 Figure 9. Zonally averaged climatological (a) barotropic zonal, (b) baroclinic zonal and (c)  
 3 baroclinic meridional winds in JJA obtained from SYNC (solid lines), CTRL (long-dashed lines)  
 4 and the NCEP-NCAR reanalysis (short-dashed line). The barotropic zonal winds are obtained by  
 5 vertically averaging the zonal winds in the troposphere (100 ~ 1000 hPa). To compute the  
 6 baroclinic zonal winds, the zonal winds are vertically averaged separately for the upper  
 7 troposphere (100 ~ 500 hPa) and for the lower troposphere (500 ~ 1000 hPa), and the latter is  
 8 subtracted from the former then divided by 2. The same methodology is used to compute the  
 9 baroclinic meridional winds.

10  
 11  
 12  
 13  
 14  
 15  
 16  
 17  
 18

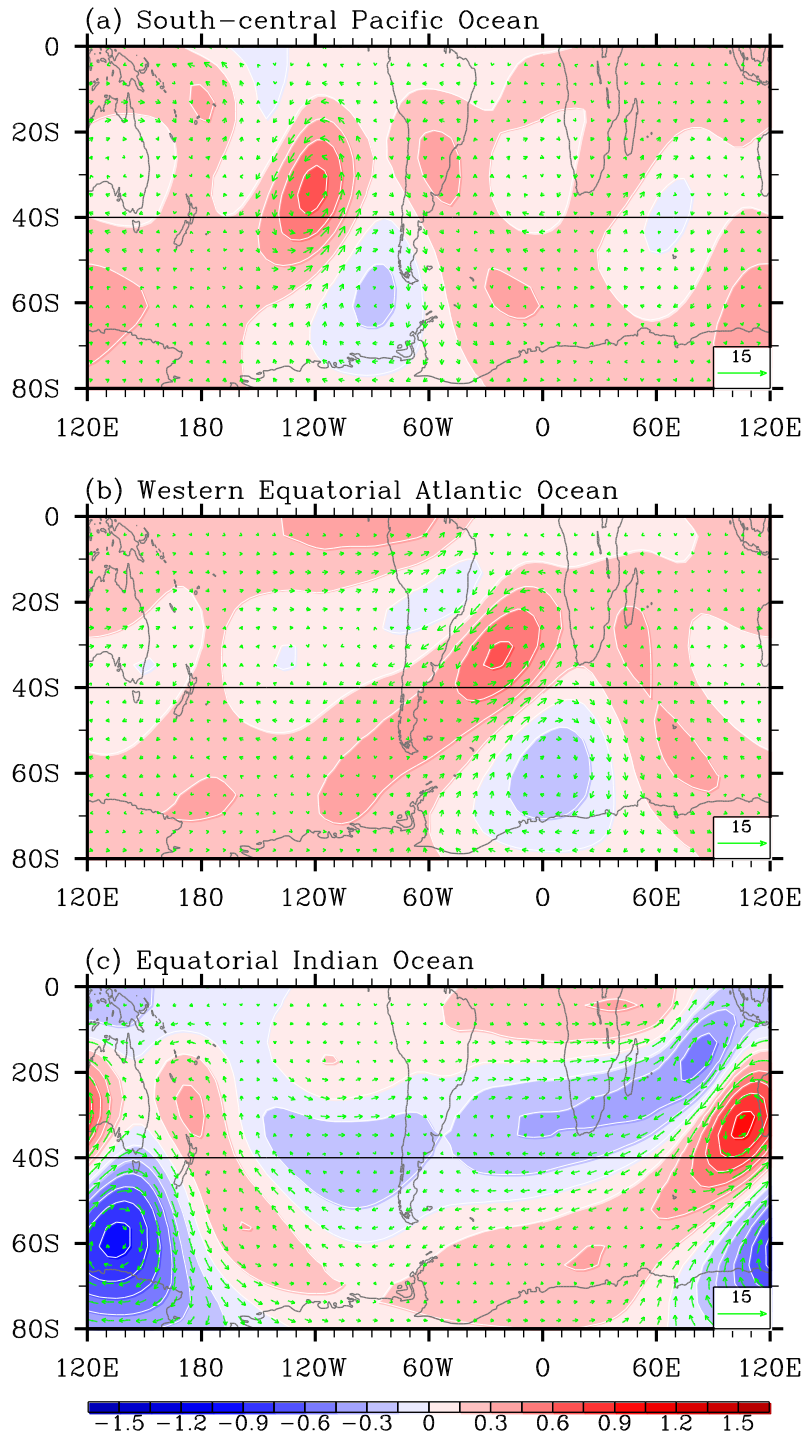
Simple Model: SFNC & Winds (JJA)



1  
2 Figure 10. Barotropic stream function and wind vector responses in the simple model  
3 experiments to the moist convective heating and cooling derived from CTRL – SYNC. The units  
4 are  $10^7 \text{ m}^2 \text{ s}^{-1}$  for stream function, and  $\text{m s}^{-1}$  for wind vector.

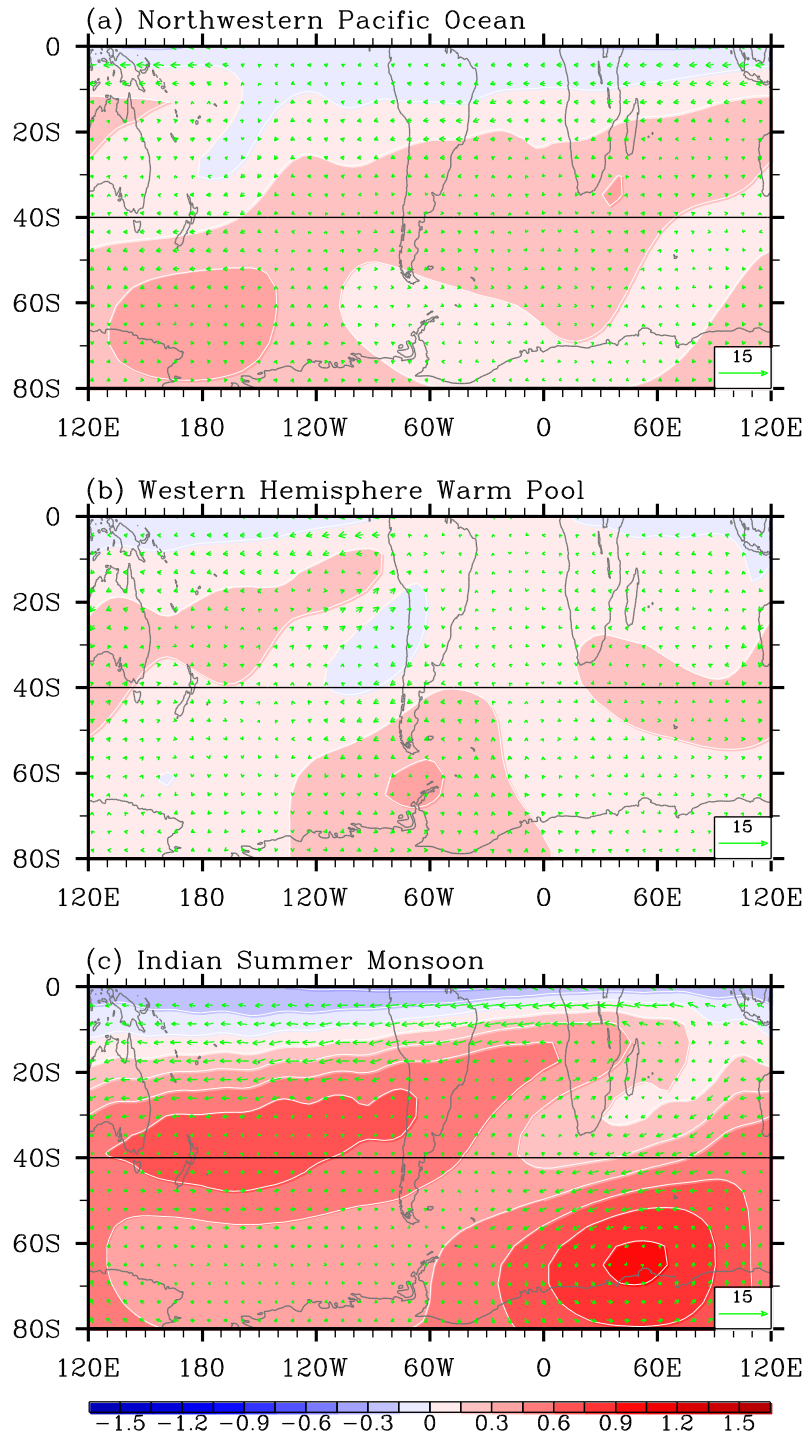
5  
6  
7  
8  
9  
10  
11  
12  
13  
14  
15  
16  
17  
18  
19  
20  
21  
22

Simple Model: SFNC & Winds (JJA)

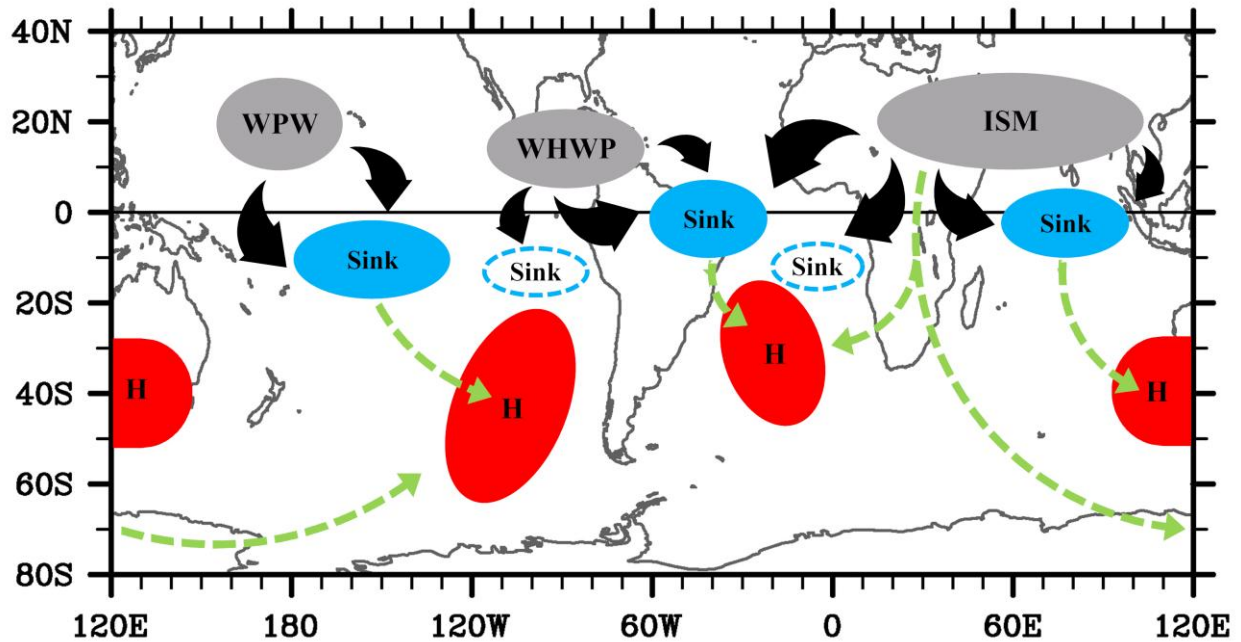


1  
2 Figure 11. Barotropic stream function and wind vector responses in the simple model  
3 experiments to diabatic cooling in (a) the central South Pacific Ocean, (b) the western equatorial  
4 Atlantic Ocean, and (c) the equatorial Indian Ocean. The units are  $10^7 \text{ m}^2 \text{ s}^{-1}$  for stream function,  
5 and  $\text{m s}^{-1}$  for wind vector.

## Simple Model: SFNC & Winds (JJA)



1  
2 Figure 12. Barotropic stream function and wind vector responses in the simple model  
3 experiments to diabatic cooling in (a) the northwestern Pacific Ocean, (b) the WHWP, and (c)  
4 the Indian summer monsoon region. The units are  $10^7 \text{ m}^2 \text{ s}^{-1}$  for stream function, and  $\text{m s}^{-1}$  for  
5 wind vector.



1  
 2 Figure 13. Sketch of the physical processes linking the major summer monsoons in the NH and  
 3 the southern subtropical anticyclones. The three regions of rising motion, the three regions of  
 4 sinking motion and the regions of southern subtropical anticyclones affected are filled with gray,  
 5 sky blue and red colors, respectively. The sinking regions in the southeastern tropical Pacific and  
 6 the southeastern tropical Atlantic are indicated by sky blue borderlines. Thick black arrows  
 7 represent divergent winds in the upper level, while light green arrows represent the paths of the  
 8 stationary barotropic Rossby waves forced by diabatic cooling over the three regions of sinking  
 9 motion and by diabatic heating in the Indian summer monsoon region.